Dalton Transactions

Accepted Manuscript

Dalton Transactions

Dynamic Article Links ►

Cite this: DOI: 10.1039/c0xx00000x

www.rsc.org/Chemcomm

COMMUNICATION

Breakdown of the geometry restriction of crystallographic site on the valence state of Eu in $CaGdAlO_4$: realization of white emission from Eu singly-doped phosphors

Yang Zhang,[a, b] , Xiaoming Liu, [c] Xuejiao Li, [a] Kai Li, [a, b] Hongzhou Lian, [a] Mengmeng Shang, [a] and Jun Lin*[, a]

Received (in XXX, XXX) Xth XXXXXXXXX 20XX, Accepted Xth XXXXXXXXX 20XX

DOI: 10.1039/b000000x

We demonstrate a strategy to manipulate the valence state of Eu in $CaGdAlO_4$ based on breakdown of the geometry restriction on the activators, which would shed light on the exploration of novel phosphors for white light emission diodes (WLEDs).

Considering the global issues of energy demand and climate deterioration, solid-state lighting (SSL) technique has become a promising alternative to conventional incandescent and fluorescent lamps on the illumination.[1-3] As the mainstream in SSL, phosphors-converted white light-emitting diodes (pc-WLEDs) have aroused fast growing interests because of their merits of high efficiency, long lifetime, environmental friendliness and energy saving.[4-7] Thus, phosphors applying to WLEDs are expected to have good performances including suitable excitation range, high quantum yield, chemical stability and low thermal quenching. So, the development of novel phosphors is critical for advanced technological applications.[8-10]

Eu, as the most widely used activator, has been playing an indispensable role in modern lighting and display fields due to the fact that both Eu^{3+} and Eu^{2+} can function as an emission center in the host lattice.[11-14] Eu^{3+} ions mainly show characteristic parity-forbidden 4f-4f transitions of $^5D_0$-^7F_J (J = 0,…,4), resulting a red emission. While the line emission and color characteristics of Eu^{3+} ions are promising for WLEDs, the low oscillator strength (about 10^{-6}) would restrict their applications due to the low absorption efficiency.[4] Eu^{2+} activated phosphors usually have broad excitation band and tunable emission colors ranging from blue to deep red because the 4f-5d transitions of Eu^{2+} ion are parity-allowed, which is more suitable for WLEDs application.[15,16] Obviously, calcination of the raw materials at high temperature under a reducing atmosphere is the easiest way to reduce Eu^{3+} to Eu^{2+}. However, the optical properties of activators are sensitive to their local environment including the crystal structure and crystallographic site size, which would hinder the valence transform feasibility to some extent.[17-21] Thus, how to break down the geometry restriction on the valence state of Eu is crucial to optimizing its optical properties for future applications. In addition, majority of research has been dedicated to using the principle of energy transfer (ET) from sensitizer (Eu^{2+} or Ce^{3+}) to activator (Tb^{3+} or Mn^{2+}) for generating white

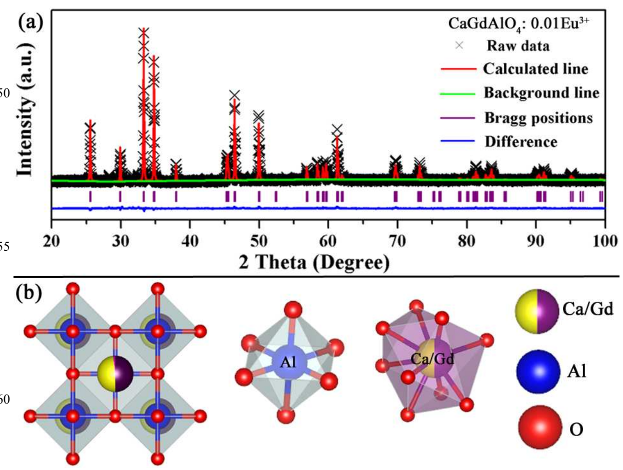

Fig. 1 (a) The Rietveld refinement to XRD pattern for $CaGdAlO_4$: 0.01Eu^{3+} sample (b) Typical crystal structure of $CaGdAlO_4$ and the Al^{3+} and Ca^{2+}/Gd^{3+} sites are depicted with six- and nine-coordination with oxygen atoms, respectively.

light. It is unavoidable that energy is consumed during the ET process, which would decrease the WLEDs efficiency.[22-25] Thus, it is a promising strategy of combine intrinsic transitions of the Eu ion from different valence states in a single host lattice directly to produce white light, based on the characteristic emissions of Eu^{2+} from blue to green and that of Eu^{3+} from orange to red.

Herein, we design and control the valence state of Eu in $CaGdAlO_4$ via release the geometry restriction on activators through the replacement of Al^{3+}-Gd^{3+} by Si^{4+}-Ca^{2+}. Rietveld refinements and detailed PL measurements have been performed on the synthesized samples, and lead to the following conclusions.[26] (1) Direct reduction of Eu^{3+} to Eu^{2+} under a reducing atmosphere is not realized in $CaGdAlO_4$ owing to the compression of Ca^{2+} sites; (2) Incorporation of Si^{4+}-Ca^{2+} into the $CaGdAlO_4$ host to replace Al^{3+}-Gd^{3+} has been attempted to expand the activator site, then fulfill the reduction of Eu^{3+} to Eu^{2+}, because Si^{4+} has a smaller radius than Al^{3+} and Ca^{2+} replacing Gd^{3+} can achieve charge compensation in the whole structure; (3) Following this mechanism, $Ca_{0.99+x}Gd_{1-x}Al_{1-x}Si_xO_4$: Eu ($x$ = 0-0.25) phosphors present tunable emission colors from coexistence luminescence of Eu^{2+} and Eu^{3+}, which holds great promise for application in WLEDs.

The samples of $Ca_{0.99+x}Gd_{1-x}Al_{1-x}Si_xO_4$: $Eu_{0.01}$ (x = 0-0.25) were prepared by conventional high temperature solid state reaction process under a reducing atmosphere of N_2 (90%) and H_2 (10%). Fig. 1a describes the results of Rietveld refinement for $CaGdAlO_4$: $0.01Eu^{3+}$ sample. The final refinement converged with weighted profiles of R_p= 2.34% and R_{wp} = 3.29%, indicating

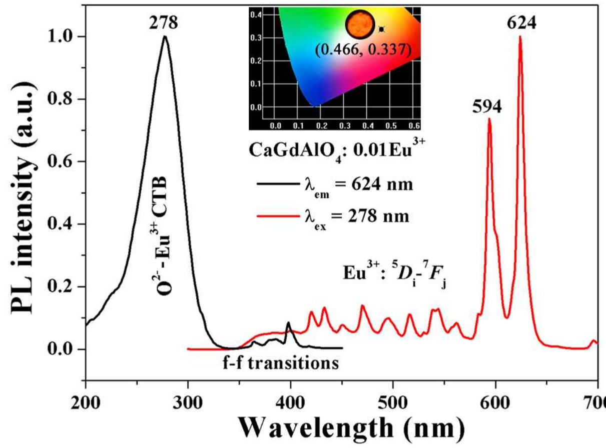

Fig. 2 The PLE and PL spectra of $CaGdAlO_4$: $0.01Eu^{3+}$ sample (λ_{em} = 624 nm, λ_{ex} = 278 nm) with corresponding photograph and CIE coordinates.

a good quality of fit. As the crystallographic data shown in Table S1, $CaGdAlO_4$ belongs to tetragonal crystal system with space group *I*4/*mmm* (No. 139). The coordination numbers (CNs) for Ca^{2+}/Gd^{3+} and Al^{3+} are 9 and 6, respectively, which means there is only one site for Ca^{2+}/Gd^{3+} to occupy with the composition ratio of 1:1. It is obvious that the $(Ca/Gd)O_9$ polyhedron is compactly surrounded by AlO_6 octahedrons to form an cage structure due to the rigid framework of $CaGdAlO_4$ as displayed in Fig. 1b.

Fig. 2 presents the photoluminescence excitation (PLE) and emission (PL) spectra of $CaGdAlO_4$: $0.01Eu^{3+}$. Monitored at 624 nm, the PLE spectrum reveals a broad band in the range of 200-350 nm related to the charge transfer band (CTB) of O_{2p}-Eu_{4f}, along with some weak peaks in the range of 350 to 450 nm due to the 4f-4f transitions of Eu^{3+}. The characteristic line emissions under 278 nm excitation can be assigned to forced electric dipole transitions ($^5D_0$-^7F_J) of Eu^{3+}, producing a red emission as the photograph and CIE coordinates shown inset of Fig. 2.[17, 27] It can be confirmed that Eu^{3+} could not be directly reduced to Eu^{2+} in $CaGdAlO_4$ system under a reducing atmosphere. Considering the local environment of activators, the Ca^{2+} site is highly compressed due to the condensed packing of AlO_6 polyhedrons. Besides, Eu^{2+} (^9r = 1.30 Å) has a larger size than Ca^{2+} (^9r = 1.18 Å). Thus, it is obvious that geometry restriction is an important factor to determine the valence state of Eu in host lattice.[17, 19]

With the aim to breakdown the limitation, Si^{4+}-Ca^{2+} has been incorporated into the $CaGdAlO_4$ host to replace Al^{3+}-Gd^{3+} , attempting to shrink the AlO_6 polyhedron, accompanied by the expansion of Ca^{2+} site, and then realize the reduction of Eu^{3+}. Firstly, Rietveld refinement has been performed to reveal the formation of a single phase in $Ca_{0.99+x}Gd_{1-x}Al_{1-x}Si_xO_4$: $Eu_{0.01}$ (CGASO: Eu, x = 0.05-0.25) as summarized in Fig. S1 and Table S2. The lattice parameters of intermediate compounds varied linearly with changing x (Fig. S2) obeying the Vegard's rule.[17] In addition, the comparison of the Raman spectra of the CGASO: Eu (x = 0, 0.10 and 0.25) samples also indicates that the crystal structure and phonon modes basically would not change with incorporation of Si^{4+}-Ca^{2+} (Fig. S3). Furthermore, the (Al/Si)-O bond length decreases with increasing x in CGASO as presented in Fig. 3. Accordingly, the (Ca/Gd)-O bond length is further elongated due to contraction of the $(Al/Si)O_6$ octahedron,

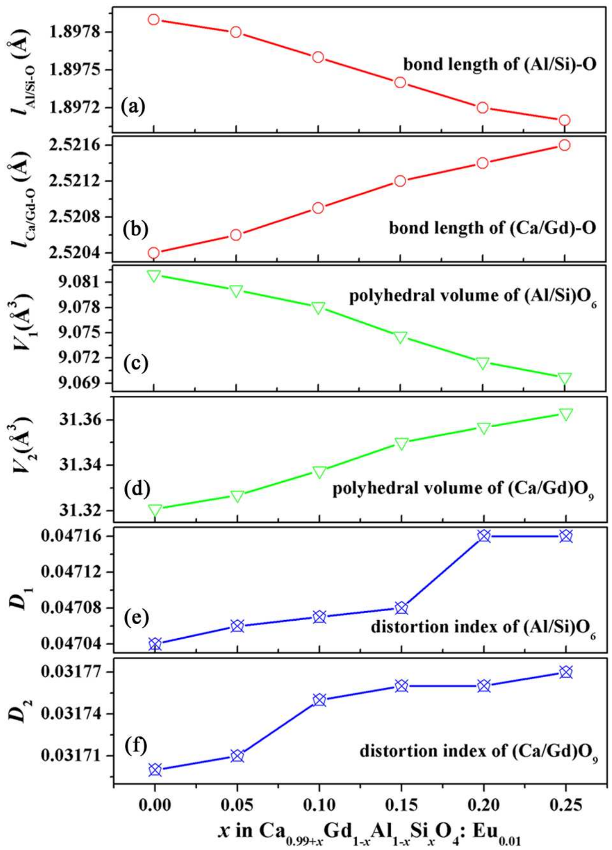

Fig. 3 The average bond length of (a) (Al/Si)-O, (b) (Ca/Gd)-O; the polyhedral volumes of (c) $(Al/Si)O_6$, (d) $(Ca/Gd)O_9$ and the related distortion index (e and f) in $Ca_{0.99+x}Gd_{1-x}Al_{1-x}Si_xO_4$: $Eu_{0.01}$ (x = 0-0.25) samples with changing x.

thus expanding the Ca^{2+} site. This is favorable for Eu^{3+} to be reduced to Eu^{2+}. Fig. 3c-f show the changing polyhedral volume and distortion index as x increases.[16, 28] Generally, the attractive force of the central cations towards the anions can be roughly evaluated by the ionic potential (φ), which can be calculated from $\varphi = Z/r$, where Z is the electric charge number of ion, and r is the ion radius (pm).[29] Once incorporating Si^{4+}-Ca^{2+} to replace Al^{3+}-Gd^{3+}, the attractive force of the Si^{4+}-O^{2-} becomes stronger compared with Al^{3+}-O^{2-}, meanwhile, the attractive force of the Ca^{2+}-O^{2-} becomes weaker compared with Gd^{3+}-O^{2-}. Thus, the geometry restriction on activators was released to some extent; as a result, a part of Eu^{3+} was successfully reduced to Eu^{2+} as the scheme shown in Fig. 4.

Taking CGASO: $Eu_{0.01}$ (x = 0.15) for example, the PLE and PL spectra were systematically studied as shown in Fig. S4. In the PLE spectrum monitored at 500 nm, a strong broad band appears around 200-450 nm with maximum at 335 nm. Accordingly, the CGASO: $Eu_{0.01}$ (x = 0.15) phosphor present a very broad symmetric emission band centred around 500 nm due to the

$4f^65d^1$-$4f^7$ transition of Eu^{2+} ions under the excitation of 335 nm.[30] As displayed in Fig. S4, a conspicuous overlap of PLE spectrum between Eu^{2+} and Eu^{3+} is found at about 300 nm. Thus,

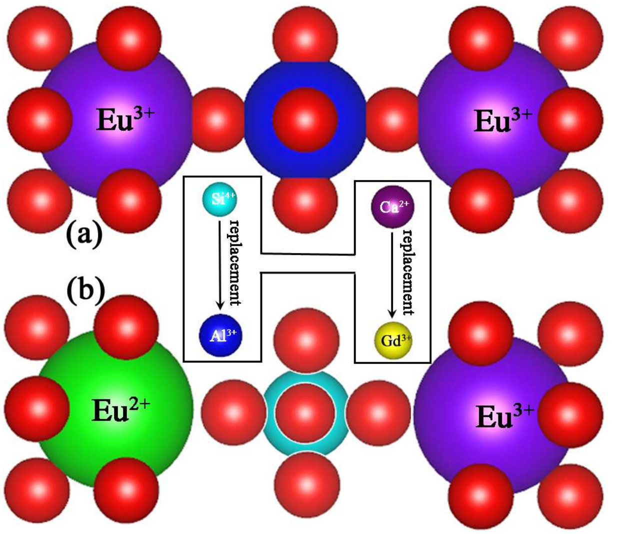

Fig. 4 Local structural coordination of Eu ions in the lattices of (a) $CaGdAlO_4$: $0.01Eu^{3+}$, (b) $Ca_{0.99+x}Gd_{1-x}Al_{1-x}Si_xO_4$: $Eu_{0.01}$ (x = 0-0.25) series. Breakdown the geometry restriction on the valence state of Eu at selected Ca^{2+} sites is proposed for the coexistence luminescence of Eu^{2+} and Eu^{3+}.

efficient PL of Eu^{2+} and Eu^{3+} can be expected to occur simultaneously in CGASO host under the 300 nm excitation, which is confirmed by the PL spectrum (the blue line) shown in Fig. S4. In addition, the decay curves of Eu^{2+} and Eu^{3+} in CGASO: $Eu_{0.01}$ (x = 0-0.25) have been performed and the life times have been summarized in Table S3. Taking CGASO: $Eu_{0.01}$ (x = 0.15) sample for simplicity, the corresponding decay curves could be well fitted to single exponential functions as $I = I_0\exp(-t/\tau)$ as presented in Fig. S5, from which the lifetimes of Eu^{2+} and Eu^{3+} were calculated to be 0.863 µs and 1.11 ms, respectively, confirming the coexistence of Eu^{2+} and Eu^{3+} activators.

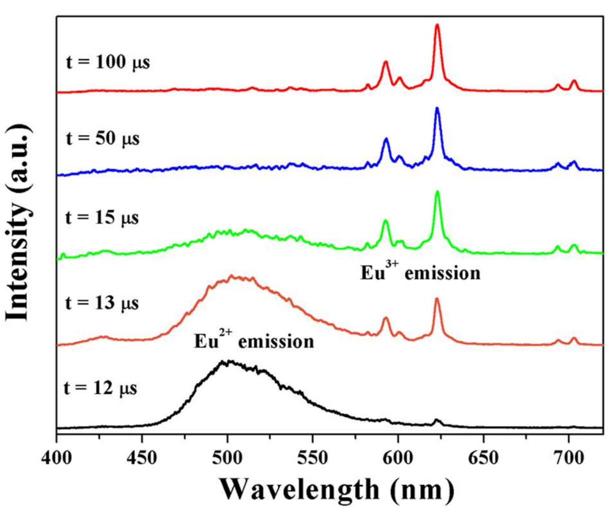

Fig. 5 The corresponding time-resolved emission spectra of $Ca_{0.99+x}Gd_{1-x}Al_{1-x}Si_xO_4$: $Eu_{0.01}$ (x = 0.15) sample (λ_{ex} = 300 nm).

Furthermore, the Eu^{3+} luminescence can be distinctly separated from Eu^{2+} from kinetic perspective through time-resolved spectra.[31] The emission spectra under short delay time (t = 12 µs) show a dominate band from Eu^{2+} ($4f^65d^1$-$4f^7$ transition) as shown in Fig. 5. The stronger Eu^{3+} ($^5D_0$ - $^7F_{0,1,2}$ transition) emission can be observed by monitoring at a longer delay time (t = 100 µs) after laser excitation along with the disappearance of Eu^{2+} emission, demonstrating that two valence states, +2 and +3, are available for Eu ions. Thus, we can conclude that partial of Eu^{3+} was successfully reduced to Eu^{2+} in CGASO: $Eu_{0.01}$ (x = 0.05-0.25) system.

Under the excitation with 300 nm, the PL spectra of CGASO: $Eu_{0.01}$ (x = 0-0.25) present both green emission of Eu^{2+} ($4f^65d^1$-$4f^7$, broadband around 500 nm) and red emission of Eu^{3+} ($^5D_0$-$^7F_{1,2}$, 594 and 624 nm) simultaneously, as shown in Fig. 6a. This result can be therefore attributed to that Eu^{3+} is partially reduced to Eu^{2+} in CGASO system with increasing x. Besides, the PL intensity of Eu^{2+} increases with increasing x in CGASO system, suggesting that the reduction process becomes easily with the gradual introduction of Si^{4+}-Ca^{2+}.[17] Due to the simultaneous presence of emission of Eu^{2+} and Eu^{3+}, the CIE coordinates of CGASO: $Eu_{0.01}$ (x = 0-0.25) upon 300 nm excitation are regularly shifted from (0.424, 0.308) to (0.282, 0.430) with changing x as depicted in Fig. 6b, and the inset shows the corresponding luminescent photographs. Especially the CIE coordinates (x = 0.372, y = 0.363) of CGASO: $Eu_{0.01}$ (x = 0.05) sample locate in white light zone, indicating the potential application for WLEDs. Under excitation with 335 nm, the PL spectra of CGASO: $Eu_{0.01}$ (x = 0-0.25) only present the broad band emission of Eu^{2+}, producing a bright green emission with the CIE (0.184, 0.474) as the photograph shown inset of Fig. 6c. Similarly, the PLE intensity gradually increases with increasing x due to the increasing level of Eu^{2+} as shown in Fig. 6d. In addition, the QY have been listed in Table S3. Furthermore, the influence of doping concentration of Eu ions on the emission intensity of the obtained $Ca_{1+x-y}Gd_{1-x}Al_{1-x}Si_xO_4$: Eu_y (x = 0.25, y = 0.005-0.07) phosphor is displayed in Fig. S6. It is apparent that the optimum doping concentration of Eu ions is y = 0.03 and the corresponding QY is 36.5% (λ_{ex} = 335 nm). Thus, this approach is promising because only a single activator, Eu, generates the multiband even a white light by optical combination of different valences of europium (Eu^{2+} and Eu^{3+} emission).

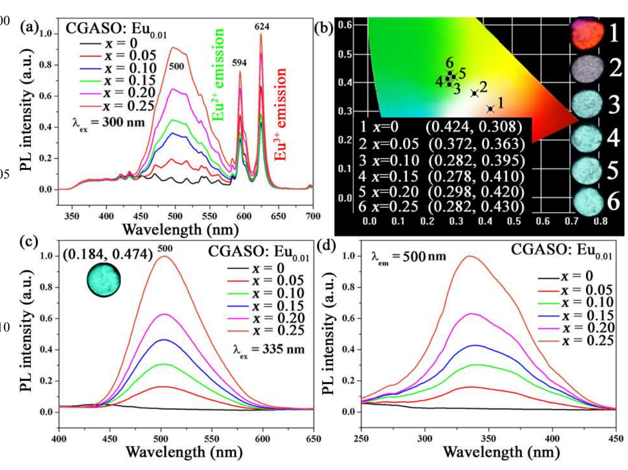

Fig. 6 The PL spectra (a) and CIE coordinates, photographs (b) of CGASO: $Eu_{0.01}$ (x = 0-0.25) samples under excitation of 300 nm, (c, d) The PL and PLE spectra of CGASO: $Eu_{0.01}$ (x = 0-0.25) samples (λ_{ex} = 335 nm and λ_{em} = 500 nm).

In summary, we presented a facile method to break down the geometry restriction on the valence state of Eu in $CaGdAlO_4$ through the replacement of Al^{3+}-Gd^{3+} by Si^{4+}-Ca^{2+}. The Rietveld refinement analysis reveals that the activator site is expanded because the average bond lengths of Al-O and Ca-O are systematically shortened and elongated simultaneously, which plays a critical role in the reduction of Eu^{3+} to Eu^{2+}. This research reveals the correlations between structure and property of host lattice, which would facilitate the discovery of novel phosphors. Furthermore, the relative intensity of Eu^{2+} and Eu^{3+} could be easily tuned through changing x in $Ca_{0.99+x}Gd_{1-x}Al_{1-x}Si_xO_4$: $Eu_{0.01}$ (x = 0-0.25), producing tunable emission colors in a wide range including white light, indicative of the potential application in WLEDs.

Financial support from the National Natural Science Foundation of China (Grants NSFC 51472234, 51202239, 51332008), the National Basic Research Program of China (Grants 2010CB327704) and the Joint Funds of the National Natural Science Foundation of China and Guangdong Province (Grant No. U1301242) are acknowledged.

Notes and references

[a] *State Key Laboratory of Rare Earth Resource Utilization, Changchun Institute of Applied Chemistry, Chinese Academy of Sciences, Changchun, 130022,P. R. China. E-mail: jlin@ciac.ac.cn;*
[b] *University of the Chinese Academy of Sciences, Beijing 100049, P. R. China*
[c] *School of Environment and Chemical Engineering, Nanchang Hangkong University, Nanchang 330063, P. R. China.*

† Electronic Supplementary Information (ESI) available: See DOI: 10.1039/b000000x/

1. J. H. Oh, S. J. Yang and Y. R. Do, *Light Sci. Appl.*, 2014, **3**, e141.
2. N. C. George, K. A. Denault and R. Seshadri, *Annu. Rev. Mater. Res.*, 2013, **43**, 481-501.
3. R. J. Xie, *J. Am. Ceram. Soc.*, 2013, **96**, 665-687.
4. J. McKittrick and L. E. Shea-Rohwer, *J. Am. Ceram. Soc.*, 2014, **97**, 1327-1352.
5. C. C. Lin and R.-S. Liu, *J. Phys. Chem. Lett.*, 2011, **2**, 1268-1277.
6. Z. J. Zhang, O. M. ten Kate, A. Delsing, M. J. H. Stevens, J. T. Zhao, P. H. L. Notten, P. Dorenbos and H. T. Hintzen, *J. Mater. Chem.*, 2012, **22**, 23871-23876.
7. E. Matioli, S. Brinkley, K. M. Kelchner, Y.-L. Hu, S. Nakamura, S. DenBaars, J. Speck and C. Weisbuch, *Light Sci. Appl.*, 2012, **1**, e22.
8. H. A. Höppe, *Angew. Chem. Int. Ed.*, 2009, **48**, 3572-3582.
9. S. Ye, F. Xiao, Y. X. Pan, Y. Y. Ma and Q. Y. Zhang, *Mater. Sci. Eng., R.*, 2010, **71**, 1-34.
10. Z.-J. Zhang, O. M. ten Kate, A. Delsing, P. Dorenbos, J.-T. Zhao and H. T. Hintzen, *J. Mater. Chem. C*, 2014, **2**, 7952-7959.
11. Y. Zhang, D. Geng, X. Kang, M. Shang, Y. Wu, X. Li, H. Lian, Z. Cheng and J. Lin, *Inorg. Chem.*, 2013, **52**, 12986-12994.
12. A. Arakcheeva, D. Logvinovich, G. Chapuis, V. Morozov, S. V. Eliseeva, J.-C. G. Bunzli and P. Pattison, *Chem. Sci.*, 2012, **3**, 384-390.
13. P. Pust, V. Weiler, C. Hecht, A. Tücks, A. S. Wochnik, A.-K. Henß, D. Wiechert, C. Scheu, P. J. Schmidt and W. Schnick, *Nat Mater*, 2014, **13**, 891-896.
14. X. Li, J. D. Budai, F. Liu, J. Y. Howe, J. Zhang, X.-J. Wang, Z. Gu, C. Sun, R. S. Meltzer and Z. Pan, *Light Sci Appl*, 2013, **2**, e50.
15. Y. Sato, H. Kato, M. Kobayashi, T. Masaki, D.-H. Yoon and M. Kakihana, *Angew. Chem. Int. Ed.*, 2014, **53**, 7756-7759.
16. K. A. Denault, J. Brgoch, M. W. Gaultois, A. Mikhailovsky, R. Petry, H. Winkler, S. P. DenBaars and R. Seshadri, *Chem. Mater.*, 2014, **26**, 2275-2282.
17. K. W. Huang, W. T. Chen, C. I. Chu, S. F. Hu, H. S. Sheu, B. M. Cheng, J. M. Chen and R. S. Liu, *Chem. Mater.*, 2012, **24**, 2220-2227.
18. C.-H. Huang, P.-J. Wu, J.-F. Lee and T.-M. Chen, *J. Mater. Chem.*, 2011, **21**, 10489-10495.
19. A. Kalaji, M. Mikami and A. K. Cheetham, *Chem. Mater.*, 2014, **26**, 3966-3975.
20. J. Park, S. J. Lee and Y. J. Kim, *Cryst. Growth Des.*, 2013, **13**, 5204-5210.
21. W.-P. Qin, Z.-Y. Liu, C.-N. Sin, C.-F. Wu, G.-S. Qin, Z. Chen and K.-Z. Zheng, *Light Sci. Appl.*, 2014, **3**, e193.
22. G. Lozano, D. J. Louwers, S. R. K. Rodriguez, S. Murai, O. T. A. Jansen, M. A. Verschuuren and J. Gomez Rivas, *Light Sci. Appl.*, 2013, **2**, e66.
23. Y. Liu, X. Zhang, Z. Hao, X. Wang and J. Zhang, *Chem. Commun.*, 2011, **47**, 10677-10679.
24. Z. Xia and R.-S. Liu, *J. Phys. Chem. C*, 2012, **116**, 15604-15609.
25. P. Ghosh, A. Kar and A. Patra, *Nanoscale*, 2010, **2**, 1196-1202.
26. A. Larson and R. Von Dreele, *Los Alamos, New Mexico* **1994**, 86-748.
27. Y. Zhang, Z. Wu, D. Geng, X. Kang, M. Shang, X. Li, H. Lian, Z. Cheng and J. Lin, *Adv. Funct. Mater.*, 2014, **24**, 6581-6593.
28. W. B. Im, N. George, J. Kurzman, S. Brinkley, A. Mikhailovsky, J. Hu, B. F. Chmelka, S. P. DenBaars and R. Seshadri, *Adv. Mater.*, 2011, **23**, 2300-2305.
29. L. Lin, X. Sun, Y. Jiang and Y. He, *Nanoscale*, 2013, **5**, 12518-12531.
30. W. B. Park, S. P. Singh and K.-S. Sohn, *J. Am. Chem. Soc.*, 2014, **136**, 2363-2373.
31. H. Xie, J. Lu, Y. Guan, Y. Huang, D. Wei and H. J. Seo, *Inorg. Chem.*, 2014, **53**, 827-834.

TOC Figure

The geometry restriction of crystallographic site on the valence state of Eu in $CaGdAlO_4$ has been overcome by the replacement of Al^{3+}-Gd^{3+} by Si^{4+}-Ca^{2+}. Tunable colors originated from the coexistence of Eu^{2+} and Eu^{3+} have been obtained in $Ca_{0.99+x}Gd_{1-x}Al_{1-x}Si_xO_4$: $Eu_{0.01}$ (x = 0-0.25) system.